NIH Public Access
Author Manuscript
Nitric Oxide. Author manuscript; available in PMC 2014 March 16.

Published in final edited form as:
Nitric Oxide. 2008 May ; 18(3): 216–222. doi:10.1016/j.niox.2008.01.002.

Quinoid radio-toxin (QRT) induced metabolic changes in mice: An *ex vivo* and *in vivo* EPR investigation

M.I. Ibragimova[a,*], **V.Yu. Petukhov**[a], **E.P. Zheglov**[a], **N. Khan**[b], **H. Hou**[b], **H.M. Swartz**[b], **G.V. Konjukhov**[a], and **R.N. Nizamov**[a]

[a]Kazan Physical-Technical Institute, Laboratory of Radiation Chemistry and Radiobiology, Sibirskii Trakt 10/7, Kazan 420029, Russia

[b]EPR Center for Viable Systems, Dartmouth Medical School, Hanover, NH 03755, USA

Abstract

Radio-toxins are toxic metabolites produced by ionizing irradiation and have toxic effects similar to those caused by direct irradiation. We have investigated the effect of a quinoid radio-toxin (QRT) obtained from γ-irradiated potato tuber on various organs in mice using *ex vivo* and *in vivo* EPR spectroscopy. Results indicate a decrease in the activity of ribonucleotide reductase enzyme in spleen of mice treated with 0.2 mg QRT. A dose of 2 mg QRT was fatal to mice within 45–60 min of treatment. Nitrosyl hemoglobin complexes α-(Fe^{2+}–NO)α-(Fe^{2+})β-(Fe^{2+})$_2$ were detected from spleen, blood, liver, kidney, heart, and lung tissue samples of mice treated with lethal doses of QRT. A significant decrease of pO_2 in liver and brain was observed after administration of QRT at the lethal dose. The time of the appearance of the nitrosyl hemoglobin complex and its intensity varied with the dose of QRT and the type of tissue. These results indicate that the effect of the QRT is more prominent in spleen and to a lesser extent in liver and blood. The QRT action at the lethal doses resulted in an increased hypoxia over time with disruption of compensatory adaptive response. The results indicate similar outcome of QRT as observed with γ-irradiation.

Keywords

Radio-toxins; Nitric oxide; Nitrosyl hemoglobin complexes; Blood; Tissue; EPR

Introduction

The need to protect animals and humans from the effects of ionizing irradiation has been recognized for a long time; this requires an understanding of the underlying mechanisms of radiation induced toxicity. While many of the effects of ionizing radiation are due to direct impact on cells resulting eventually in cell death, there is evidence that some of the effects may be due to post-irradiation radio-toxinemia and auto-immune responses arising from the radiolysis of proteins, polypeptides, and amino acids [1]. There is a wide range of toxic compounds, termed as radio-toxins (RTs), which can induce such effects [1,2].[1] The toxicity induced in the first few hours after irradiation is biologically active in regard to damage to the cell genome and bio-membranes damage. RTs are also able to increase the radiobiological effects by secondary damage of cell functions [2].

© 2008 Published by Elsevier Inc.

[*]Corresponding author. Fax: +7 843 272 5075. ibragimova@kfti.knc.ru (M.I. Ibragimova).

[1]The appearance of different kinds of radio-toxins in biological objects after γ-irradiation has been widely investigated by scientists in Russia. There are many experimental data testifying the influence of RT obtained from irradiated objects on metabolic process in plants and animals. We did not find any reference on the investigation of these effects in other laboratories from the rest of the world.

NIH-PA Author Manuscript
NIH-PA Author Manuscript
NIH-PA Author Manuscript

NIH-PA Author Manuscript

NIH-PA Author Manuscript

NIH-PA Author Manuscript

Known RTs are quinoid radio-toxins (products of the oxidation of polyphenols particularly *o*-quinones stabilized by peptides), lipid RT (products of the oxidation of unsaturated higher fatty acids), derivatives of histidine, different kinds of oxyaldehydes and others [1,2]. Radio-toxins can be generated from a variety of biological systems including plants and microorganisms. It is known that the effects of RT can be similar to classical direct radiation damage: mitotic delay, mitotic block, chromosomal aberrations, and cell death [1]. Therefore, the study on the effects of RT on rodents could provide important insights into the mechanism of action of ionizing irradiation, and this information could be potentially used to develop processes to modify radiation induced damage in medicine, agriculture, and in other fields.

Different biological and immune-chemical methods have been used to investigate radio-toxins but their applications are limited by rather low sensitivity. One of the modern physical methods for the investigation of metabolic changes in biological objects under ionizing radiation is electron paramagnetic resonance (EPR) spectroscopy [3].

Using EPR spectroscopy, it has been established that NO-synthase is upregulated in X-ray [4] and γ-irradiated animals [5–7]. However, the amount of endogenous NO depends on the dose, and perhaps the most important is the dose rate. For NO detection in liver [4,5] and bile [6] after irradiation with doses ranging from 6 to 50 Gy and dose rates of 0.6–3.7 Gy/min, different types of spin traps have been used. On the other hand, the direct *ex vivo* EPR measurements revealed that the doses higher than 2 Gy with dose rate of 7.3 cGy/min in the early post-irradiation period (from 2 to 6 h) induce α-(Fe^{2+}–NO)α-(Fe^{2+})β-(Fe^{3+})$_2$ complexes in blood and spleen [7].

Earlier [8,9], the effect of quinoid radio-toxin (QRT) which is an ethanolic extract obtained from γ-irradiated potato tubers on living organism has been investigated. The consequences of QRT and γ-irradiation action on hemopoiesis and pathology changes in tissue are similar: they cause stimulation effects at low doses and depressive toxic effect at high doses [8]. Therefore, QRT is radiomimetic imitating radiation injury of macroorganism. QRT has been used for hyperimmunization of animal donors as well [8,9]. The antiradiotoxic serum sampled from these animals was applied as a specific immunocompetent component in the production of the antibody erythrocyte preparation for an oblique hemagglutination test (OHT) [9]. We demonstrated the usage of OHT for the early diagnosis of the acute radiation disease caused by γ-irradiation of different animals (mice, rats, rabbits, sheep, pigs) [8].

Our earlier *in vitro* EPR investigation has unambiguously shown that QRT is a strong hemolytic agent similar to 1% HCl and it causes irreversible changes in the blood [10]. A nearly 300-times increase of the methemoglobin signal from the blood samples was observed during 5 h after QRT treatment. However, in living organisms the actual biological processes and response to toxins can be quite different than *in vitro* results. In this study, we have investigated the metabolic changes in mice treated with QRT at different doses using *ex vivo* and *in vivo* EPR to understand the effect of QRT on live animals.

Materials and methods

QRT preparation

QRT was obtained from potato tubers (“Nevskii” strain) irradiated by γ-rays of ^{60}Co with a dose of 400 Gy. A more detailed procedure of QRT preparation is published elsewhere [11]. According to [1] QRTs have a complex chemical composition. They contain the oxidation products of quinoid and semiquinoid nature. The homogenate was prepared after 24 h incubation of irradiated tubers at 20 °C. Radio-toxin was then extracted from an ethanolic homogenate. Then it was neutralized by 0.1M KOH to pH 7.4. The yield of radio-toxin from

NIH-PA Author Manuscript

NIH-PA Author Manuscript

NIH-PA Author Manuscript

raw materials was 2.5 ± 0.5 ml for 100 g of initial potato tubers. The biological activity of QRT was estimated by measuring the hemolysis of ram erythrocytes.

An extract from the unirradiated potato tubers prepared by the same procedure was used as a control.

Sample and animal preparation

All animal procedures were approved by the Institutional Animal Care and Use Committee of Dartmouth Medical School. For each experiment, more than five Male Balb C mice (Charles River Laboratories, Wilmington, MA) and the control group of untreated mice were used.

Solutions containing 10 mg QRT/ml or extract from unirradiated potato tubers were injected in the intraperitoneal cavity of the mice with doses of 0.1, 0.15 or 0.2 ml. The injection of 0.2 ml preparation containing 2 mg of QRT resulted in the lethality of mice in 45–60 min, while 0.15 ml containing 1.5 mg QRT was lethal in 2–3 h after injection. For *ex vivo* EPR experiments, the animals were sacrificed at 0.5, 0.75, 1-h time points after QRT treatments. An injection of 0.1–0.2 ml preparation containing no more than 1 mg QRT did not lead to the death of the animal. After injection of 0.2 ml diluted solution containing 0.2 mg QRT/mouse, the animals were sacrificed at 0.5, 0.75, 1, 4 and 8-h time points after treatments.

The blood and tissue samples of spleen, liver, kidney, heart, and lung were collected and then immediately frozen in liquid nitrogen for *ex vivo* EPR measurements. Heparin was used in blood samples to prevent the blood from clotting. EPR measurements were performed at cryogenic temperatures in a 9.5 GHz (X-band) Varian EPR spectrometer with SHF power being 50 mW and modulation amplitude of 1 G. For quantitative measurements, the same volume of the frozen blood and the equal amount of the tissue were used in all the experiments. After each EPR measurement, the signal from the standard sample (anthracite with $g = 2.0030$) mounted in the other part of resonator was recorded. For quantitative analysis, the amplitude of the EPR signals was normalized using the amplitude of the standard signal.

EPR oximetry measurements were carried out on a 1.2 GHz EPR spectrometer with a microwave bridge and an external loop resonator specially designed for *in vivo* experiments [12,13]. Oxygen-sensitive lithium phthalocyanine (LiPc) crystals were synthesized at the EPR Center for Viable Systems (Dartmouth Medical School, Hanover, NH). LiPc crystals have been used extensively to measure partial pressure of oxygen (pO_2) in various tissues [14–17]. The EPR spectra from LiPc reflect pO_2 of the tissue on the surface of the crystals. This oximetry probe has a single sharp EPR line with a good sensitivity of the line width to pO_2 [14–17]. Approximately 40 μg of LiPc crystals was injected in the liver or brain tissue using a 23 gauge needle and plunger. The mice were anesthetized using 2.5% isoflurane with 26% FiO_2 (the fraction of inspired oxygen in a gas) and aseptic procedures were used for LiPc implantation in tissue as per the guidelines of Institutional Animal Care and Use Committee of Dartmouth Medical School, Hanover, NH. The animals were allowed to recover for 3–5 days and the QRT/pO_2 experiments were performed on day 6 after LiPc implantation. For EPR measurements, the mouse were anesthetized using 1.5% isoflurane with 26% FiO_2 and the body temperature was maintained at 37 ± 1 °C during the experiments using a warm water pad and warm air blower. After a 30 min pO_2 baseline measurement, the mice were treated with QRT and the changes in the tissue pO_2 of liver or brain tissue were continuously measured for 1–3 h.

NIH-PA Author Manuscript

NIH-PA Author Manuscript

NIH-PA Author Manuscript

Results

Results of 0.2 mg QRT/mouse treatment

Any pathological changes in internal of mice after QRT injection at low doses were not found. No detectable changes in the EPR spectra of the liver, kidney or blood samples were observed in 8 h after QRT treatment. However, certain changes in the *ex vivo* EPR spectra from the spleen sample in the region of $g \sim 2$ were registered (see Fig. 1). A decrease in the signal intensity of the EPR spectra from spleen tissue samples collected at 30 min, 4 h, or 8 h post QRT was observed. The EPR parameters of the doublet are $g = 2.008$ and hyperfine splitting $a = 20$ G. This signal is assigned to the active form of enzyme ribonucleotide reductase (RR) containing a radical of the tyrosine amino acid residue [18]. No significant change in the liver and brain tissue pO_2 was registered during 24 h after treatment with doses of up to 1 mg QRT per mouse (Fig. 2).

Treatment of mice with lethal doses of QRT

Treatment of mice with QRT at LD_{50} leads to the depression of hemopoiesis (Table 1), the reduction of erythrocytes hemolytic stability, and the increase of malonic dialdehyde in the liver. In addition, at the LD_{100} the hemorrhagic syndrome was observed, such as, hyperemia of internal blood vessels, point hemorrhage in the mucosa of bowels, kidney and liver, pulmonary edema, and changes in structure and size of the spleen.

Ex vivo EPR analysis of the tissue samples revealed additional EPR lines. The EPR signals (in the spectra region $g \sim 2$) registered from spleen samples collected at 30, 45 and 60 min after QRT treatments are shown in Fig. 3. A wide EPR line with a distinct triplet hyperfine structure ($g \sim 2.01$ with hyperfine splitting of 17 G) was detected and the intensity of this signal increased with time after QRT injection. The spectroscopic parameters suggest that this signal is likely to be hemoglobin–NO complexes formed as a result of the interaction of deoxyhemoglobin with nitric monoxide [19,20]. No MetHb ($g \sim 6$) signal was registered from spleen samples.

Ex vivo EPR spectra from *liver* (curve 1), *kidney* (curve 2), *heart* (curve 3), and *lung* (curve 4) of dead mice after 2 mg QRT injection are shown in Fig. 4. An EPR signal with a *g*-factor of 2.01 and hyperfine splitting of 17 G was detected in all the samples, but the signal intensity varied in different tissues. These spectra are similar to that observed from the spleen and are assigned to the hemoglobin–NO complexes. However, the shape of absorption lines from the heart and lung indicated an overlap of this EPR signal with the typical signals of these tissues. No lines at $g \sim 6$ were registered.

EPR spectra from hemoglobin–NO complexes were also observed from the blood samples of mice treated with QRT. A typical EPR spectrum (in the region of $g \sim 2$) after 30 min of QRT (0.2 ml preparation with 2 mg QRT) injection is shown in Fig. 5. We did not detect any MetHb signal from blood samples.

EPR spectra from tissue and blood samples of mice treated with the extract from unirradiated potato tubers were similar to those of untreated mice.

Effect of lethal dose QRT on tissue pO_2 measured by EPR oximetry

The dynamics of pO_2 changes in liver and brain of mice before and after lethal doses of QRT are shown in Fig. 6. The tissue pO_2 of liver increased by a factor of 1.5–2 during 20–30 min after injection of 1.5 mg QRT and then decreased continuously until the animal died. Prior to death, the pO_2 level was 2–3 times less than that of the observed baseline tissue pO_2. However, at a higher dose of QRT, the tissue pO_2 decreased immediately after QRT

NIH-PA Author Manuscript

NIH-PA Author Manuscript

NIH-PA Author Manuscript

treatment. The changes in the brain tissue pO_2 were similar to that observed in the liver, but the effects were not as drastic as those observed in the liver (Fig. 6B).

Discussion

Ex vivo EPR analysis and direct *in vivo* EPR pO_2 measurements allowed us to investigate the dynamics of metabolic changes in mice after injection of QRT at different doses.

The low-dose QRT (0.2 mg/mouse) did not lead to any significant changes in *ex vivo* and *in vivo* EPR spectra from the tissues investigated, except from the spleen samples. Results indicate a gradual reduction of the intensity of RR signal which is likely due to the suppression of RR synthesis occurring at 8 h after QRT treatment. Much attention has been given to the EPR spectrum of RR observed from the spleen due to its important role in the replication of DNA. The linear dependence between the intensity of this signal and RR activity was reported earlier [3,18]. The depression of RR activity in the cells for a long period of time affects the efficacy of repair and replication of deoxyribonucleotides [21]. A similar reduction of RR activity was observed from the spleen of mice at 12 h after γ-irradiation with a dose of 6 Gy and a dose rate of 3.5 Gy/min [3,22]. Thus, our results of time-dependent changes in the intensity of the RR signal indicate that one of the consequences of the low-dose QRT treatment is the effect on the repair of DNA.

The *in vivo* EPR measurements of QRT action at high doses clearly demonstrate the hypoxia progression in liver and brain tissues. In particular, at the dose of 1.5 mg/mouse (resulted in death with in 2–3 h), the liver pO_2 increased by 45 ± 10% during the first 30 min, and then the pO_2 started to decrease with an approximate rate of 0.4 ± 0.1 mm Hg/min. The increase of QRT dose to 2 mg/mouse (mice died within 45–60 min) led to immediate suppression of the oxygen delivery in liver and brain tissues (i.e. decrease in tissue pO_2). The rate of pO_2 decline in the liver occurred at approximately 0.6 ± 0.1 mm Hg/min. These results indicate that at the dose of 2 mg QRT/mouse, the hypoxic conditions arise in the whole organism almost immediately after the injection of the preparation.

Moreover at lethal doses, the *ex vivo* EPR measurements revealed the formation of Hb–NO complexes which is due to excess generation of NO. The appearance of the wide EPR line at $g \sim 2$ in *ex vivo* EPR spectra and the absence of the signal from MetHb (at $g \sim 6$) suggest the formation of α-Hb–NO complexes (α-(Fe^{2+}–NO)α-(Fe^{2+})β-(Fe^{2+})$_2$) [19,23]. It has been established that both the time of the signal appearance and its intensity depend on the type of tissue. At all doses of QRT (lethal and low), the spleen appears to be the most sensitive organ in the animals investigated. At a QRT dose of 2 mg/mouse, endogenous nitric oxide is registered in spleen samples after 20–30 min, and its concentration increased with time. After 30–40 min, α-(Fe^{2+}–NO)α-(Fe^{2+})β-(Fe^{2+})$_2$ complex appeared in spectra recorded from samples of blood and liver, while in other tissues (kidney, heart, lung), a high concentration of NO was observed much later, just before animal death.

Multicomponent chemical composition of QRT invokes the complex action on the total organism. Our previous *in vitro* EPR measurements [10] have shown that the mixture of QRT with blood in ratio 1:15 led to an increase of MetHb signal intensity by 3–4 times in 2–3 min and by 300 times in 5 h as well as to the destruction of Fe^{3+}-transferrin and the appearance of unspecific form of iron (similar to 1% HCl). It should be noted a peculiarity of QRT action on blood *in vitro*. After 1 h incubation the EPR absorption signal in spectra region of $g \sim 6$ is the superposition at least of three lines unidentified at this time. Thus, the action of QRT on blood *in vitro* involves the oxidation of heme's Fe^{2+} and destruction of Fe-containing proteins. In *in vivo* experiments, it appears that the lethal dose of QRT administration into the intraperitoneal cavity of the mice leads to the strong oxidation of Fe-

NIH-PA Author Manuscript

NIH-PA Author Manuscript

NIH-PA Author Manuscript

containing proteins in the whole organism. It is obvious that this process must lead to the activation of defense response of the organism. We believe that the launch of the compensatory adaptive response is confirmed by the pO_2 increase during ~30 min after the QRT injection with the dose of 1.5 mg/mouse. At the dose of 2 mg/mouse the compensatory adaptive response is disrupted immediately after QRT administration. Surprisingly, the signals at $g \sim 6$ were not observed in *ex vivo* EPR spectra of tissue and blood at 30 min after administration of QRT with dose of 2 mg/mouse whereas Hb–NO complexes were observed.

We propose the following mechanism of a robust increase in Hb–NO signal after QRT injection with the lethal dose.

Immediately after 2 mg/mouse QRT injection, the oxidation of heme Fe^{2+} to Fe^{3+} occurs which leads to a decrease in oxygen supply to the tissue. Under enhanced hypoxia (see Fig. 6) endogenous nitrite can be implicated as a source of bioavailable NO [24]. The most likely mechanism is the reaction of nitrite with deoxyhemoglobin (Fe^{2+}) reducing nitrite to NO. This reaction leads to the formation of NO, MetHb (Fe^{3+}) and OH. NO then reacts with deoxyhemoglobin (Fe^{2+}) yielding iron-nitrosyl-hemoglobin. Under hypoxic conditions, the concentration of the oxyhemoglobin decreases and the intermediates of the reaction of nitrite with oxyhemoglobin do not oxidize heme iron in nitrosyl hemoglobin. It leads to a decrease of NO release from iron-nitrosyl as observed in our experiments. The absence of the MetHb signals can be explained by the fact that NO reversibly binds to MetHb and forms diamagnetic nitrosylmethemoglobin, which eventually autoreduces by a first order reaction ($k' \sim 10^{-3}\ s^{-1}$; $t_{1/2} \sim 12$ min) to a paramagnetic species Hb–NO [25,26].

The comparative data of *ex vivo* EPR investigation of metabolic changes in animals treated with QRT and γ-irradiation are summarized in Table 2. Data show the effect of the suppression of the active form of enzyme ribonucleotide reductase in the spleen which is observed with both, the treatment with QRT (0.2 mg/mouse) or the total γ-irradiation with dose of 6 Gy and dose rate of 3.5 Gy/min. At higher doses (more than 1.5 mg/mouse) of QRT, the NO generation is upregulated and is detected by direct *ex vivo* EPR. Such effect is also observed after the γ-irradiation with a dose of 500 Gy at high dose rates [3] or irradiation with dose of 6 Gy at smaller dose rates [7]. In the spleen, the intensities of EPR signals from Hb–NO complexes at 45 min after QRT (2 mg/mouse) and at 6 h after irradiation with dose of 6 Gy and dose rate of 7.3 cGy/min [7] are similar. However, two differences exist. First, after irradiation the MetHb concentration increased while after QRT treatment this signal was absent. Second, in the case of QRT injection with doses more than 1.5 mg/mouse the compensatory adaptive response is disrupted, and the concentration of Hb–NO increased continuously. At 2 mg QRT/mouse, the nitrosyl hemoglobin complex concentration in the spleen increased more than 3 times (see spectra 2 and 3 in Fig. 3) at 15–20 min before animal death.

In summary, our results indicate a similar response after treatment with QRT as that observed with γ-irradiation. Therefore, QRT could be used to investigate the effect of radiation induced injury *in vivo*.

Acknowledgments

This work was supported by ISTC's Grant #1901 "Elaboration of immune-chemical and physical test-systems for express diagnosis and prognosis of the radiation injury" and used the facilities of EPR Center for Viable Systems (P41 EB002032, NIH).

NIH-PA Author Manuscript

NIH-PA Author Manuscript

NIH-PA Author Manuscript

References

1. Kusin, AM.; Kopylov, VA. Radio-toxins. Nauka; Moscow: 1983. (in Russian)
2. Kudryashov, Yu B. Main principals in radiobiology. Radiobiol Radioecol. 2001; 41:521–547. (in Russian).
3. Pulatova, MK.; Rikhireva, GT.; Kuropteva, ZV. Electron paramagnetic resonance in molecular radiobiology. Energoatomizdat; Moscow: 1989. (in Russian)
4. Nakagawa H, Ikota N, Ozawa T, Kotake Y. Dose- and time dependence of radiation induced nitric oxide formation in mice as quantified with electronic paramagnetic resonance. Nitric Oxide. 2001; 5:47–52. [PubMed: 11178936]
5. Mikoyan VD, Voevodskaya NV, Kubrina LN, Malenkova IV, Vanin AF. Exogenous iron and γ-irradiation induce synthesis of NO-synthase in liver of mice. Biochemistry. 1994; 59:732–737. (in Russian).
6. Kotake Y, Moore DR, Sang H, Reinke LA. Continuous monitoring of *in vivo* nitric oxide formation using EPR analysis in bile flow. Nitric Oxide. 1999; 3:114–122. [PubMed: 10369181]
7. Ibragimova MI, Yu V, Petukhov, Zheglov EP, Konjukhov GV, Nizamov RN. Investigation of metabolic changes in blood and tissue of mice γ-irradiated with sublethal doses by direct observation of EPR signals from Hb–NO complexes. Appl Mag Reson. 2005; 29:589–596.
8. Project summary for unrestricted distribution of ISTC #1901, Elaboration of the immune-chemical and physical test-systems for express-diagnosis and prognosis of the radiation injury.
9. Ravilov, AZ.; Nizamov, RN.; Konjuchov, GV.; Kurbangaleev, YaM; Petukhov, VYu. The method of production of the antibody erythrocyte preparation for radiation injury diagnostics. Patent of the Russian Federation No. 2240137. 2004. (in Russian)
10. Ibragimova MI, Yu V, Petukhov, Zheglov EP, Konjukhov GV, Nizamov RN. *In vitro* and *ex vivo* EPR investigation of metabolic changes in blood under the action of radio-toxins obtained from irradiated potato tubers. Radiats Biol Radioecol. 2004; 44:529–534. (in Russian). [PubMed: 15571040]
11. Avilov, VM.; Ravilov, AZ.; Kirshin, VA.; Nizamov, RN.; Konjuchov, GV.; Akmullina, NV.; Kurbangaleev, YaM; Chernova, RV.; Vetrov, VP. The method of diagnostics of radiation injury and the method of the production of preparation for diagnostics. Patent of the Russian Federation No. 2145712. 2000. (in Russian)
12. Swartz HM, Walczak T. Developing in vivo EPR Oximetry for clinical use. Adv Exp Med Biol. 1998; 454:243–252. [PubMed: 9889898]
13. Hirata H, Walczak T, Swartz HM. Electronically tunable surface-coil-type resonator for L-Band EPR spectroscopy. J Magn Reson. 2000; 142:159–167. [PubMed: 10617447]
14. Swartz HM, Clarkson RB. The measurement of oxygen *in vivo* using EPR techniques. Phys Med Biol. 1998; 43:1957–1975. [PubMed: 9703059]
15. Liu KJ, Gast P, Moussavi M, Norby SW, Vahidi N, Walczak T, Wu M, Swartz HM. "Lithium phthalocyanine": A probe for electron paramagnetic resonance oximetry in viable biological systems. Proc Natl Acad Sci USA. 1993; 90:5438–5442. [PubMed: 8390665]
16. Jiang J, Nakashima T, Liu KJ, Goda F, Shima T, Swartz HM. Measurement of pO_2 in liver using EPR oximetry. J Appl Physiol. 1996; 80(2):552–558. [PubMed: 8929598]
17. Khan N, Williams BB, Hou H, Li H, Swartz HM. Repetitive tissue pO_2 measurements by electron paramagnetic resonance oximetry: current status and future potential for experimental and clinical studies. Antioxid Redox Signal. 2007; 9(8):1169–1182. [PubMed: 17536960]
18. Thelander L, Reichard P. Reduction of ribonucleotides. Ann Rev Biochem. 1979; 48:133–158. [PubMed: 382982]
19. Kosaka H, Sawai Y, Sakaguchi H, Kumura E, Harada N, Watanabe M, Shiga T. EPR spectral transition by arteriovenous cycle in nitric oxide hemoglobin of cytokine-treated rats. Am J Physiol. 1994; 266:C1400–C1405. [PubMed: 8203503]
20. Yonetani T, Tsuneshige A, Zhou Y, Chen X. Electron paramagnetic resonance and oxygen binding studies of α-nitrosyl hemoglobin. J Biol Chem. 1998; 32:20323–20333. [PubMed: 9685383]

NIH-PA Author Manuscript

NIH-PA Author Manuscript

NIH-PA Author Manuscript

21. Snyder RD. Deoxyribonucleoside triphosphate pools in human diploid fibroblasts and their modulation by hydroxyurea and deoxynucleosides. Biochem Pharmacol. 1984; 33:1515–1524. [PubMed: 6732868]

22. Avakyan MA, Sharygin VL, Pulatova MK, Efremova OI, Todorov IN. Iron-sulphur containing centers of respiratory chain, ribonucleotide reductase activity and macromolecule biosynthesis in mouse spleen during acute radiation disease. Radiobiology. 1986; 26:626–646. (in Russian). [PubMed: 2430311]

23. Jaszewski AR, Fann JC, Chen Y, Sato K, Corbett J, Mason RP. EPR spectroscopy studies on the structural transition of nitrosyl hemoglobin in the arterial-venous cycle of DEANO-treated rats as it relates to the proposed nitrosyl hemoglobin/nitrosothiol hemoglobin exchange. Free Radic Biol Med. 2003; 36:444–451. [PubMed: 12899946]

24. Grubina R, Huang Z, Shiva S, Joshi MS, Azarov I, Basu S, Ringwood LA, Jiang A, Hogg N, Kim-Shapiro DB, Gladwin MT. Concerted nitric oxide formation and release from the simultaneous reactions with nitrite with deoxy and oxyhemoglobin. J Biochem Chem. 2007; 282:12916–12927.

25. Hall D, Buettner GR. *In vivo* spin trapping of nitric oxide by heme: electron paramagnetic resonance detection *ex vivo*. Meth Enzym. 1996; 268:188–192. [PubMed: 8782584]

26. Hall D, Buettner GR, Gisolfi CV, Matthes RD. *In vivo* detection of nitric oxide and NO_x using *ex vivo* electron paramagnetic resonance spectroscopy. Microchem J. 1997; 59:165–170.

NIH-PA Author Manuscript
NIH-PA Author Manuscript
NIH-PA Author Manuscript

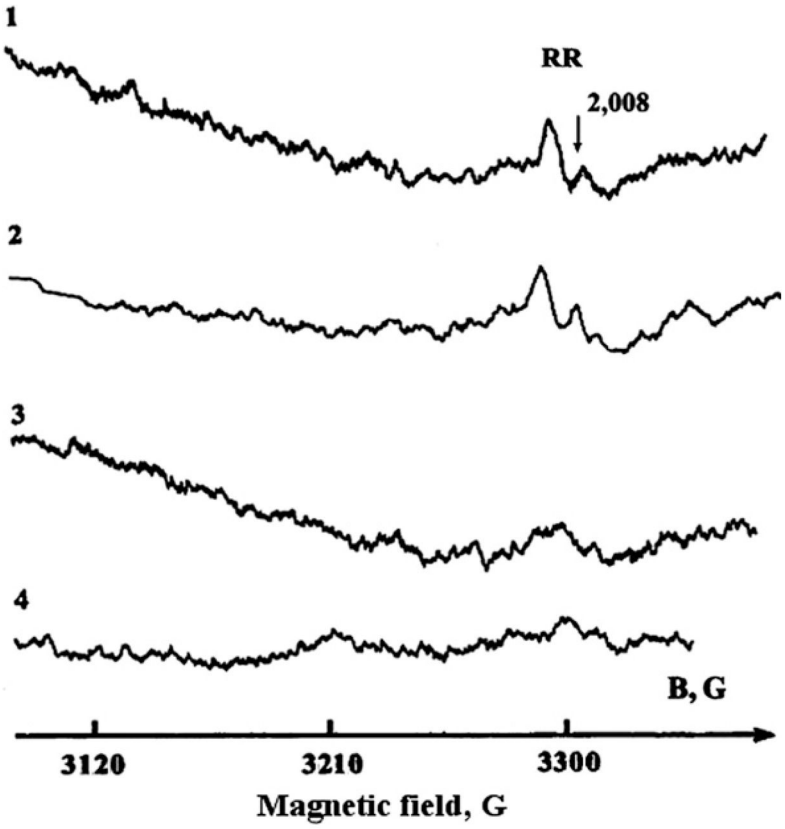

Fig. 1.
Time dependence of EPR spectra recorded from spleen of mice after intraperitoneal injection of 0.2 ml of preparation containing 0.2 mg QRT/mouse. Spectrum 1, from intact mice; 2, after 30 min; 3, after 4 h; and 4, after 8 h post QRT injection. All the spectra were recorded at 77 K.

NIH-PA Author Manuscript
NIH-PA Author Manuscript
NIH-PA Author Manuscript

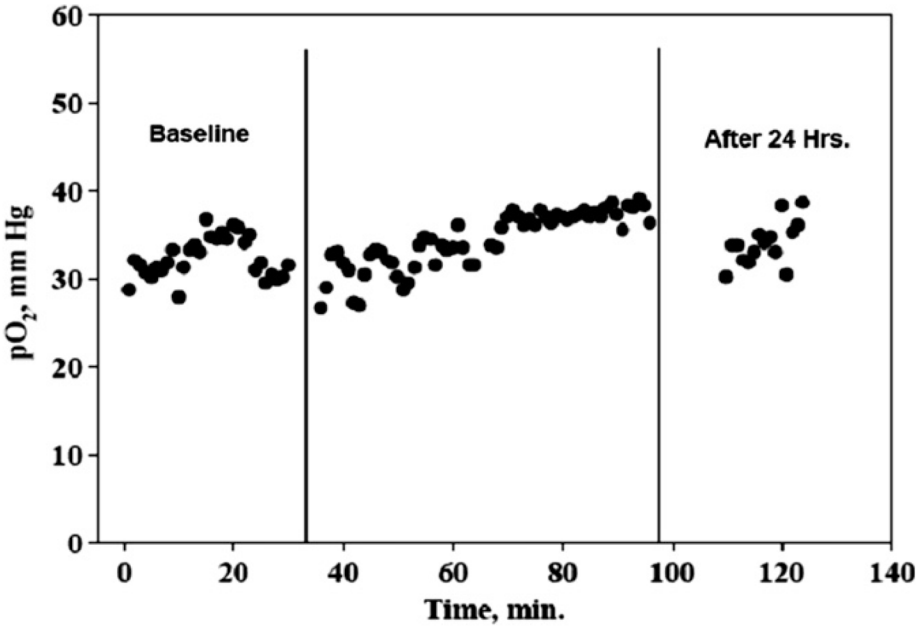

Fig. 2.
Changes of pO_2 level in liver of mouse before and after intraperitoneal injection of preparation containing 1 mg QRT.

NIH-PA Author Manuscript
NIH-PA Author Manuscript
NIH-PA Author Manuscript

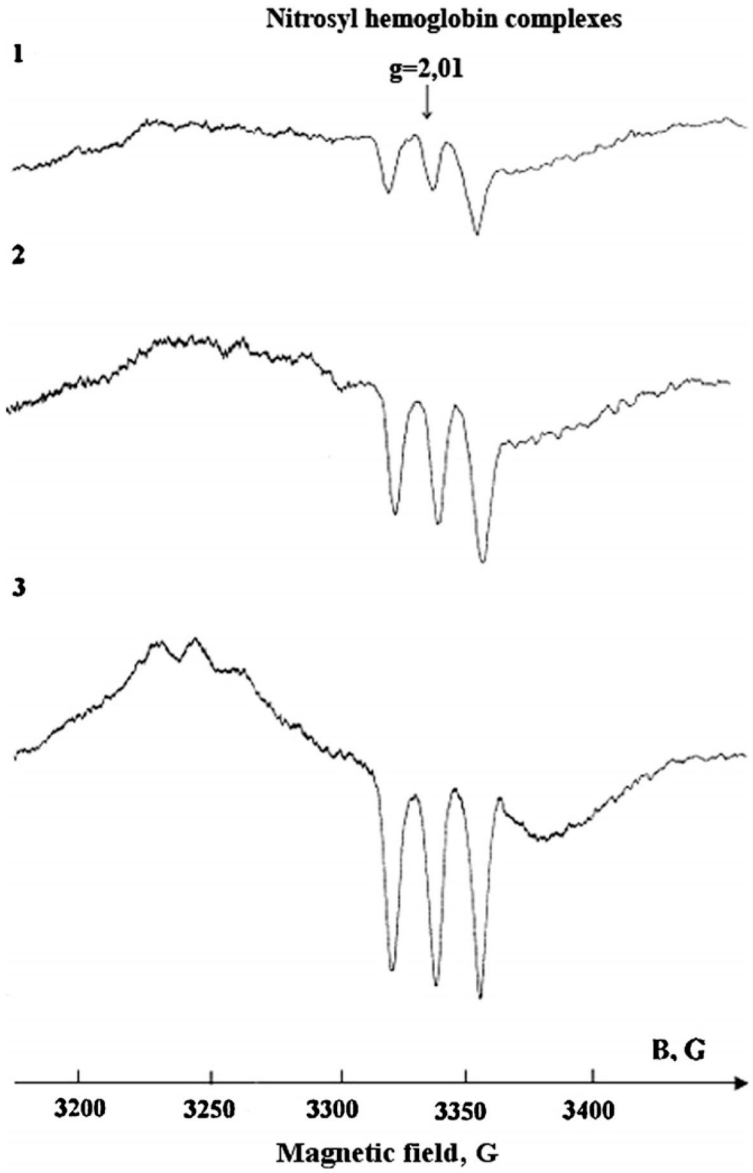

Fig. 3.

Ex vivo EPR spectra observed from spleen samples after; (1), 30 min; (2), 45 min; and (3), 60 min after injection of 0.2 ml preparation containing 2 mg of QRT. All the spectra were recorded at 77 K.

NIH-PA Author Manuscript

NIH-PA Author Manuscript

NIH-PA Author Manuscript

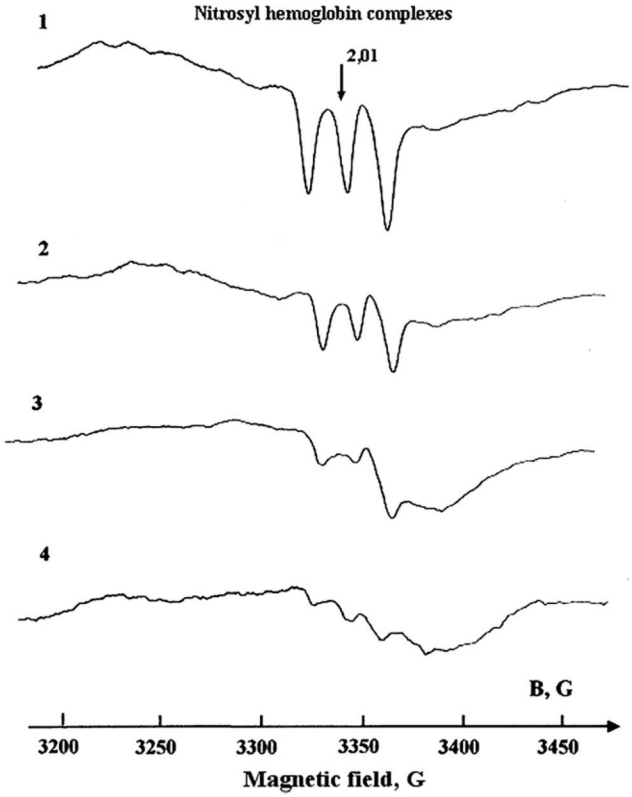

Fig. 4.

Ex vivo EPR spectra obtained from (1), liver; (2), kidney; (3), heart, and (4), lung samples of dead mice in 60 min after injection of 0.2 ml preparation containing 2 mg of QRT. All the spectra were recorded at 77 K.

NIH-PA Author Manuscript

NIH-PA Author Manuscript

NIH-PA Author Manuscript

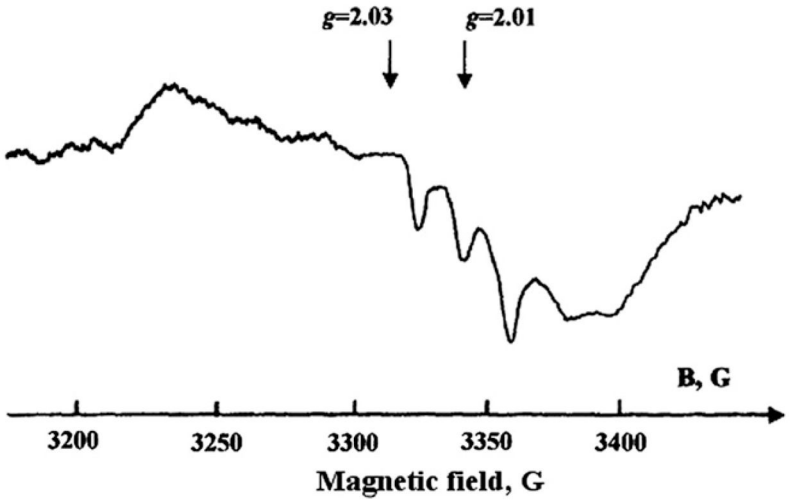

Fig. 5.

Ex vivo EPR spectra recorded at 77 K from blood samples of mouse in 40 min after injection of 0.2 ml preparation containing 2 mg of QRT.

NIH-PA Author Manuscript

NIH-PA Author Manuscript

NIH-PA Author Manuscript

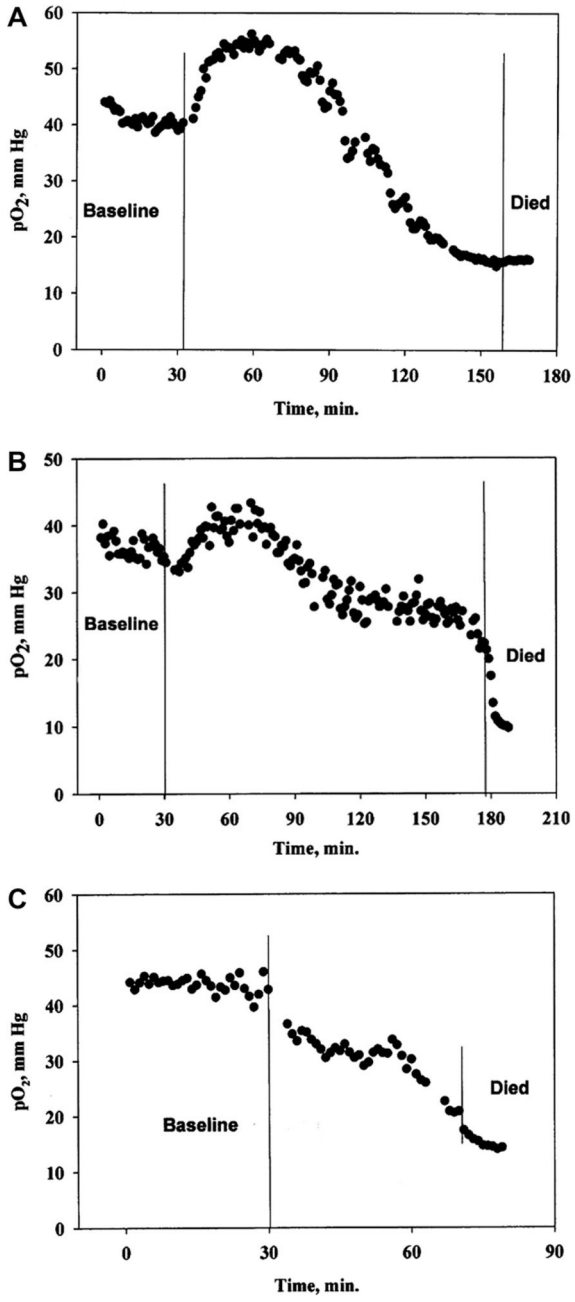

Fig. 6.

The dynamics of pO_2 changes in liver (A and C) and brain (B) of mice before and after injection of preparation with the lethal doses containing 1.5 mg QRT (A and B) and 2 mg QRT (C) per mouse.

NIH-PA Author Manuscript

NIH-PA Author Manuscript

NIH-PA Author Manuscript

Table 1

Blood count of mice 1 day after QRT injection at LD_{50}

Blood count	Control	After QRT
Myelokaryocytes, × 10^6/femur	22.5 ± 2.35	2.25 ± 0.37
Leukocytes, × 10^3/mm^3	4.62 ± 0.64	0.29 ± 0.04
Neutrophils, × 10^3/mm^3	0.91 ± 0.11	0.08 ± 0.02
Lymphocytes, × 10^3/mm^3	3.26 ± 0.44	0.21 ± 0.03
Thrombocytes, × 10^3/mm^3	0.39 ± 0.55	0.04 ± 0.05
Erythrocytes, × 10^3/mm^3	5.95 ± 0.05	3.53 ± 0.11
Hemoglobin, g/l	14.9 ± 0.13	10.2 ± 0.30

NIH-PA Author Manuscript

NIH-PA Author Manuscript

NIH-PA Author Manuscript

Table 2

Effects in tissue of laboratory animals under the QRT and γ-irradiation impacts

Effects registered from *ex vivo* EPR spectra	**QRT injection**	**γ-Irradiation**
The suppression of the active form of the enzyme ribonucleotide reductase *in spleen*	In 8 h after injection of preparation containing 0.2 mg QRT/mouse	In 12 h after γ-irradiation with dose of 6 Gy at the dose rate of 3.5 Gy/min [22]
Enhanced generation of nitric oxide *in spleen* and blood	In 30 min after injection of preparation containing 2 mg QRT/mouse. Oxidation of Fe^{2+}–heme up to Fe^{3+} is not revealed	In ~2 h after irradiation with doses of ≥2 Gy with dose rate of 7.3 cGy/min. Oxidation of Fe^{2+}–heme up to Fe^{3+} is revealed [7] After irradiation with dose of 500 Gy; the value of dose rate is not presented [3]